REPORT SD-TR-86-49
REISSUE A

Dynamic Fatigue of Ultralow-Expansion Glass for Space Mirrors, Reissue A

D. J. SPEECE
Materials Sciences Laboratory
Laboratory Operations
The Aerospace Corporation
El Segundo, CA 90245

30 October 1988
(Supersedes and replaces SD-TR-86-49
dated 8 August 1986.)

Prepared for

SPACE DIVISION
AIR FORCE SYSTEMS COMMAND
Los Angeles Air Force Base
P.O. Box 92960
Los Angeles, CA 90009-2960

This report was submitted by The Aerospace Corporation, El Segundo, CA 90245, under Contract No. F04701-85-C-0086 with the Space Division, P.O. Box 92960, Worldway Postal Center, Los Angeles, CA 90009-2960. It was reviewed and approved for The Aerospace Corporation by R. W. Fillers, Director, Materials Sciences Laboratory. Lt Donald Thoma, SD/YXTI, was the Air Force project officer.

This report has been reviewed by the Public Affairs Office (PAS) and is releasable to the National Technical Information Service (NTIS). At NTIS, it will be available to the general public, including foreign nationals.

This technical report has been reviewed and is approved for publication. Publication of this report does not constitute Air Force approval of the report's findings or conclusions. It is published only for the exchange and stimulation of ideas.

DONALD THOMA, Lt, USAF
Project Officer
SD/YXTI

JOSEPH HESS, GM-15
Director, AFSTC West Coast Office
AFSTC/WCO OL-AB

UNCLASSIFIED

SECURITY CLASSIFICATION OF THIS PAGE

REPORT DOCUMENTATION PAGE

1a. REPORT SECURITY CLASSIFICATION Unclassified	1b. RESTRICTIVE MARKINGS
2a. SECURITY CLASSIFICATION AUTHORITY	3. DISTRIBUTION/AVAILABILITY OF REPORT Approved for public release; distribution unlimited.
2b. DECLASSIFICATION/DOWNGRADING SCHEDULE	
4. PERFORMING ORGANIZATION REPORT NUMBER(S) TR-0086(6409-11)-1, Reissue A	5. MONITORING ORGANIZATION REPORT NUMBER(S) SD-TR-88-49, Reissue A
6a. NAME OF PERFORMING ORGANIZATION The Aerospace Corporation Laboratory Operations 6b. OFFICE SYMBOL (*If applicable*)	7a. NAME OF MONITORING ORGANIZATION Space Division
6c. ADDRESS (*City, State, and ZIP Code*) El Segundo, CA 90245-4691	7b. ADDRESS (*City, State, and ZIP Code*) Los Angeles Air Force Base Los Angeles, CA 90009-2960
8a. NAME OF FUNDING/SPONSORING ORGANIZATION 8b. OFFICE SYMBOL (*If applicable*)	9. PROCUREMENT INSTRUMENT IDENTIFICATION NUMBER F04701-85-C-0086
8c. ADDRESS (*City, State, and ZIP Code*)	10. SOURCE OF FUNDING NUMBERS PROGRAM ELEMENT NO. / PROJECT NO. / TASK NO. / WORK UNIT ACCESSION NO.

11. TITLE (*Include Security Classification*)
Dynamic Fatigue of Ultralow-Expansion Glass for Space Mirrors, Reissue A

12. PERSONAL AUTHOR(S)
Speece, Dana J.

13a. TYPE OF REPORT	13b. TIME COVERED	14. DATE OF REPORT (*Year, Month, Day*)	15. PAGE COUNT
	FROM _____ TO _____	1988 October 30	31

16. SUPPLEMENTARY NOTATION

17. COSATI CODES		
FIELD	GROUP	SUB-GROUP

18. SUBJECT TERMS (*Continue on reverse if necessary and identify by block number*)
Ceramics, Mirrors
Fatigue, Ultralow-expansion (ULE) glass
Fracture

19. ABSTRACT (*Continue on reverse if necessary and identify by block number*)

Ultralow-expansion (ULE) glass is one of the primary materials used for space mirrors because its SiO_2-TiO_2 composition has a very low coefficient of thermal expansion. Several problems with cracking of this material in the Defense Satellite Program (DSP) led to the conclusion that insufficient design information was available to ensure reliability of the mirror structure. Accordingly, the Materials Sciences Laboratory of The Aerospace Corporation undertook an investigation into the fracture behavior of ULE glass for space mirrors.

Dynamic fatigue experiments were performed on two sets of samples (optically polished and lightly ground) to characterize the fracture behavior of this material in a humid environment. As expected, the flaw size distribution affects the expected lifetime at a given stress and failure probability. In addition, it is shown that the polished material is apparently less sensitive to subcritical crack growth than the unpolished glass.

20. DISTRIBUTION/AVAILABILITY OF ABSTRACT	21. ABSTRACT SECURITY CLASSIFICATION
☐ UNCLASSIFIED/UNLIMITED ☒ SAME AS RPT. ☐ DTIC USERS	Unclassified
22a. NAME OF RESPONSIBLE INDIVIDUAL	22b. TELEPHONE (*Include Area Code*) / 22c. OFFICE SYMBOL

DD FORM 1473, 84 MAR 83 APR edition may be used until exhausted. All other editions are obsolete.

SECURITY CLASSIFICATION OF THIS PAGE

UNCLASSIFIED

PREFACE

The data base for ultralow-expansion glass, available in the open literature, is limited. Therefore, all published data must be correct. A close review of the original work by one of the authors uncovered an error in the stressing rate values that were reported. The corrections resulted in small numerical changes in the tables, figures, and text of the superseded document, as follows:

- Corrected stress rates are a factor of 10 lower than the old values.
- The slope decreased and the intercept increased in Fig. 3; the changed values are used in Eqs. (5), (5a), and (5b).
- The calculated values for N and B increased 1 to 2%.
- The constants in the time-to-failure Eqs. (6a) and (6b) changed.
- The predicted breaking stresses in Figs. 4 through 6 increased 15 to 20%.

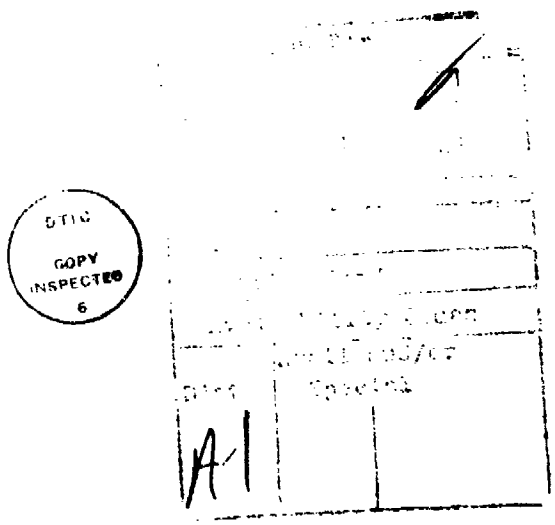

CONTENTS

FIGURES

TABLES

I. INTRODUCTION

Ultralow-expansion (ULE) glass has many space applications, including telescopes and optical mirrors. ULE glass is desirable primarily because of its low coefficient of thermal expansion. Like all brittle materials, it is subject to catastrophic failure under a variety of conditions; these conditions include impact loading, stresses in service, and stresses during manufacturing and polishing operations. During the polishing operation, the material is frequently exposed to water, which may facilitate subcritical crack growth. A previous study[1] of ULE glass examined the crack propagation of this material using crack velocity versus fracture toughness (K_I) data and calculated the corresponding proof-test design diagram. The purpose of this report is to define better the effects of flaw population and subcritical crack growth on this material.

The flaw population and its relation to failure of the material can generally be described in terms of a two-parameter Weibull distribution,[2] so that the probability of failure of the component, F, is

$$F = 1 - \exp\left[-K_A\left(\frac{\sigma_f}{\sigma_0}\right)^m\right] \tag{1}$$

where K_A is a constant related to the area (for surface flaws) under stress, the loading geometry σ_f is the fracture stress, and m and σ_0 are constants related to the distribution of strengths. Both σ_0 and m are empirically determined from a plot of $\ln(\ln 1/1 - F)$ versus $\ln \sigma_f$, where the strength data have been rank-ordered from lowest to highest. The higher the value of m, the narrower the strength distribution.

Methods of combining Weibull statistics with data on static or dynamic fatigue data to yield predictions of the lifetime of brittle materials under various environmental conditions have been demonstrated in Refs. 3 and 4. (For completeness, the derivations are provided in Appendix A.) The relevant equation is

$$\ln t_f = \ln B + \frac{N-2}{m_i}\left[\ln\left(\ln \frac{1}{1-F}\right) + m_i \ln \sigma_{0i}\right] - N \ln \sigma_a \tag{2}$$

where B is a constant that takes into account the loading geometry, the flaw geometry, the critical fracture toughness, and the exponent for the rate of crack growth; m_i is the Weibull modulus in a fast-fracture inert environment; $\ln \sigma_{0i}$ is the intercept of the $\ln(\ln 1/1 - F)$ versus $\ln \sigma_f$ plot in a fast-fracture inert environment; N is the exponent for the rate of crack growth; and σ_a is the applied stress. In general, the constants B and N must be determined experimentally for the set of environmental conditions of interest. The reliability of these determinations is critical to their ultimate use[5] and will be discussed later in the report.

Silicate glasses are generally subject to subcritical crack growth under certain environmental conditions,[1,6-9] especially in the presence of water or environmental humidity. Since ULE glass is subjected to water during grinding and polishing, and has exhibited subcritical crack growth, it is appropriate to examine more closely its behavior when different flaw populations are present. The dynamic fatigue experiments were chosen to provide the environmental parameters because the time required for this type of experiment is significantly less than that needed for the other possible experiments.

II. EXPERIMENTAL PROCEDURE

Test specimens 0.5 × 1.0 × 6.0 cm were sawn from billets of a two-component silicate glass[a] containing 7.5% TiO_2 and 92.5% SiO_2. The samples were prepared in two ways. One group was lightly ground on four sides with 100-μm Al_2O_3; the second group was ground with three grits of Al_2O_3, the final grit being 9 μm. The tensile test surface of the second group was polished to mirror quality. The edges of all samples were beveled to reduce the incidence of corner failures. The samples were stored at ambient conditions (22°C, < 50% relative humidity) prior to testing.

Modulus of rupture (MOR) was measured in three-point bending and with a test span of 3.8 cm on a commercial testing machine.[b] Testing was performed in a closed chamber, in either high relative humidity (>90%) or dry-nitrogen atmospheres. Inert-strength data were provided by testing at high stress rates in the nitrogen atmosphere. Samples were exposed to the nitrogen atmosphere for 15 min before being loaded to fracture. Testing in the high-humidity environment was performed at three stress rates, also after ~ 15 min of exposure.

The dimensions of each bar and the load at failure were recorded and used to calculate the MOR. Fracture surfaces were examined in the optical microscope to locate the fracture origins.

---

[a]Code 7971, Corning Glass Works, Corning, NY.

[b]Instron Corp., Canton, MA.

III. RESULTS

The modulus of rupture was calculated from the dimensions and load at failure; the average MOR and standard deviation for each of the sample sets are shown in Table 1. (The complete set of data is included in Appendix B.) The data were rank-ordered from low to high, and the probability of failure F was computed by

$$F = \frac{n - 0.5}{N} \tag{3}$$

where n is the rank of the sample and N is the total number of samples in the set. The data for the unpolished materials are shown in Fig. 1 as $\ln(\ln 1/1 - F)$ versus $\ln \sigma_f$ (MOR). Data for the polished materials are plotted in Fig. 2 in the same fashion. The rank-ordered data were then fit to a straight line of the form

$$\ln(\ln \frac{1}{1 - F}) = m \ln \sigma_0 + m \ln \sigma_f \tag{4}$$

The values of the Weibull modulus m and the intercept $\ln \sigma_0$ are also given in Table 1. The data from both sets of material indicate a multimodal flaw distribution.[10] Since the correlation coefficient of the linear regression was greater than 0.8 in all cases, the two-parameter Weibull distribution was accepted as valid for those tests.

In order to obtain the values of B and N in Eq. (2), the median fracture stress and stress rate data for the high-humidity samples were fit to a straight line by

$$\ln \hat{\sigma}_f = a_0 + a_1 \ln \dot{\sigma} \tag{5}$$

where

$$a_0 = \frac{\ln[B(N + 1)] + (N - 2) \ln \sigma_i}{N + 1} \tag{5a}$$

Table 1. Results of Three-Point-Bend Dynamic Fatigue Tests

$\dot{\sigma}(\frac{MPa}{s})$	Number of Samples	Environment and Surface Finish	$\hat{\sigma}_f$(MPa)	m	$\ln \sigma_0$ (σ_0 in Pa)	R^2
0.12	25	H_2O lightly ground	43.97	5.67	17.74	0.91
0.12	25	H_2O polished	67.38	4.13	18.05	0.89
1.23	25	H_2O lightly ground	44.89	6.47	17.76	0.82
1.23	25	H_2O polished	76.59	6.75	18.21	0.97
12.3	25	H_2O lightly ground	59.09	8.97	17.92	0.94
12.3	25	H_2O polished	79.70	4.94	18.02	0.95
12.3	25	N_2 lightly ground	65.03	5.75	18.03	0.95
12.3	25	N_2 polished	83.72	5.05	18.35	0.96
147	14	N_2 lightly ground	71.03	11.91	18.11	0.95
347	8	N_2 lightly ground	56.20	6.95	17.98	0.88

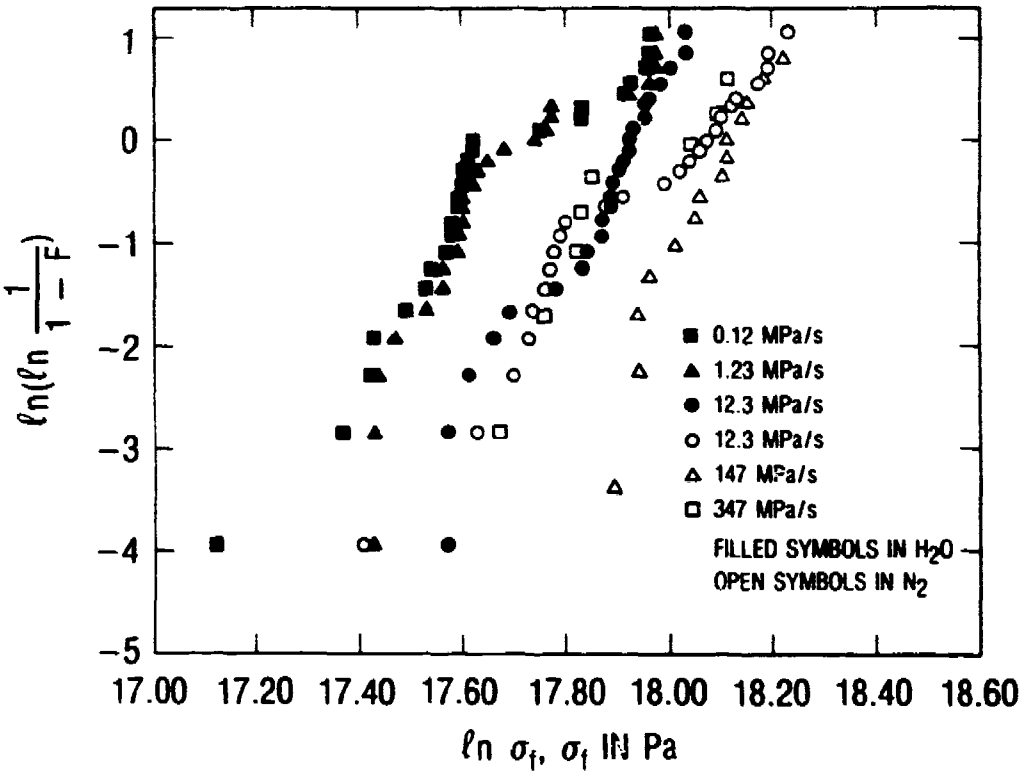

Fig. 1. Dynamic Fatigue Strength Distributions for Unpolished ULE Glass

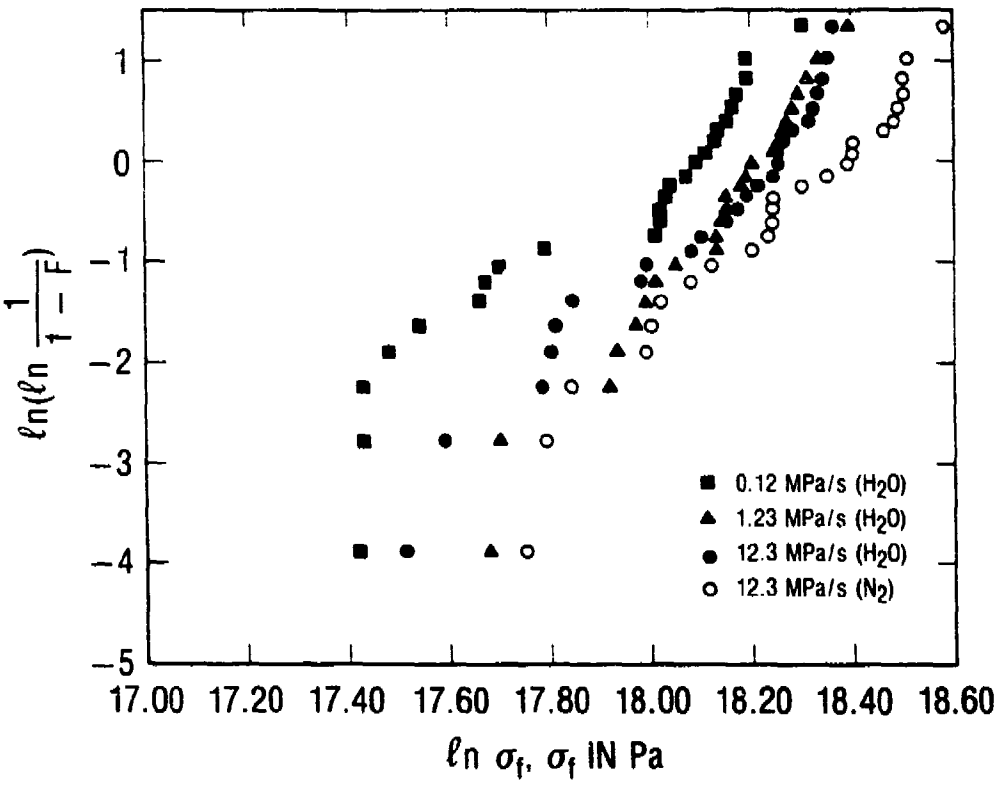

Fig. 2. Dynamic Fatigue Strength Distributions for Polished ULE Glass

and

$$a_1 = \frac{1}{N + 1} \tag{5b}$$

These data are shown in Fig. 3. Using the values obtained for a_0, a_1, and $\hat{\sigma}_f$, N, and $\ell n\ B$ were calculated for the unpolished and polished samples and are given in Table 2.

The time-to-failure for various values of F and σ_a can now be computed from Eq. (2). The equation reduces to

$$\ell n\ t_f = 266.01 + 2.26\ \ell n(\ell n \frac{1}{1 - F}) - 14.97\ \ell n\ \sigma_a \tag{6a}$$

for the unpolished material and

$$\ell n\ t_f = 506.44 + 5.13\ \ell n(\ell n \frac{1}{1 - F}) - 27.90\ \ell n\ \sigma_a \tag{6b}$$

for the polished material. Figure 4 shows the results of these calculations for three values of F (0.2, 0.01, and 0.001) for the unpolished material, whereas Fig. 5 shows the same information for the polished glass. For both materials, the result is three parallel lines, one for each value of F. Also shown on the graph are the maximum allowable stresses for a lifetime of 10 yr. There is a significant difference between the allowable stress level for the polished material and that for the unpolished material. This difference is shown more clearly in Fig. 6 for a fixed probability of failure. It is obvious that as the allowable failure rate increases, the maximum allowable stress also increases.

Before the data developed in this study can be used, several factors must be considered. The first factor is the degree to which the sample flaw population resembles the actual flaw population in service; in the present case, the flaw population of unpolished but lightly ground material is expected to resemble a roughly ground mirror blank, and that of the polished material represents the finished blank. The second factor

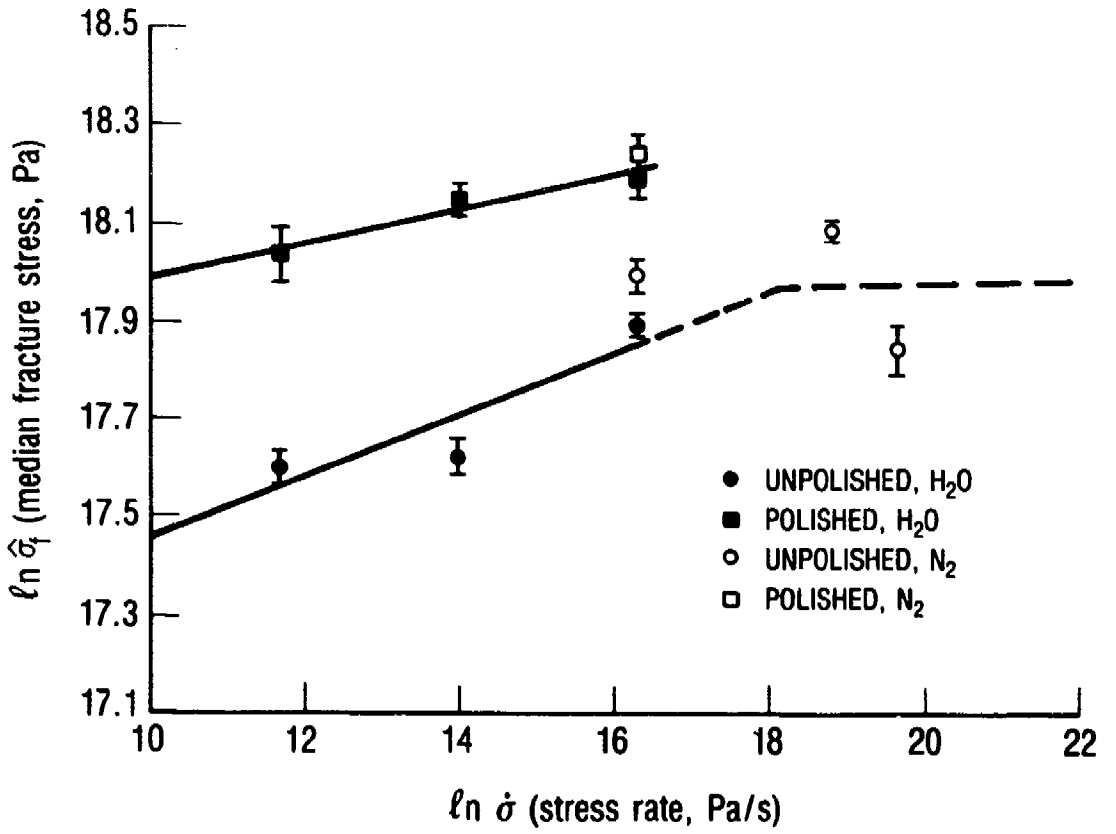

Fig. 3. Median Strength $\hat{\sigma}_f$ as a Function of Stress Rate $\dot{\sigma}$ for Polished and Unpolished ULE Glass

Table 2. Fatigue Parameters for Lightly Ground and Polished ULE Glass Materials

Material	N	ℓn B	R^2
Lightly ground	14.97	32.16	0.800
Polished	27.90	31.17	0.924

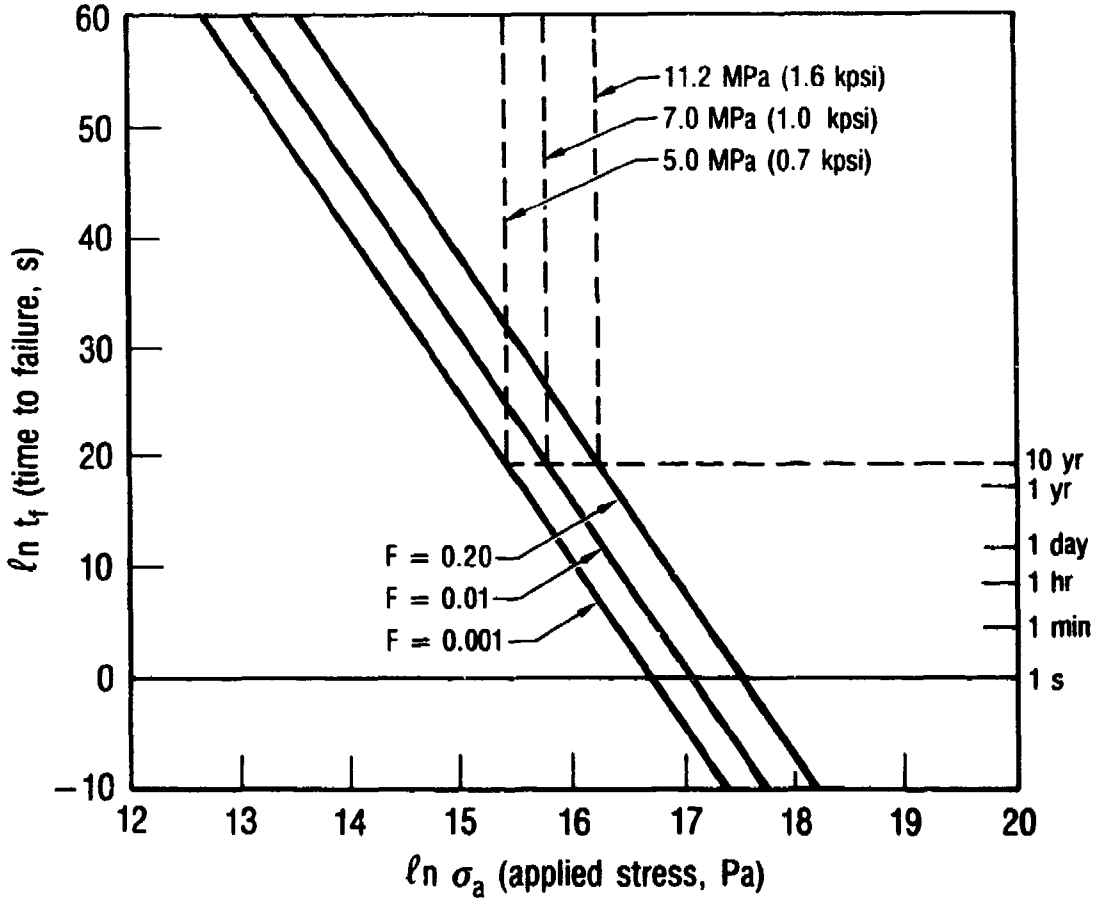

Fig. 4. Design Diagram for Unpolished ULE Glass, Based on Dynamic Fatigue Data

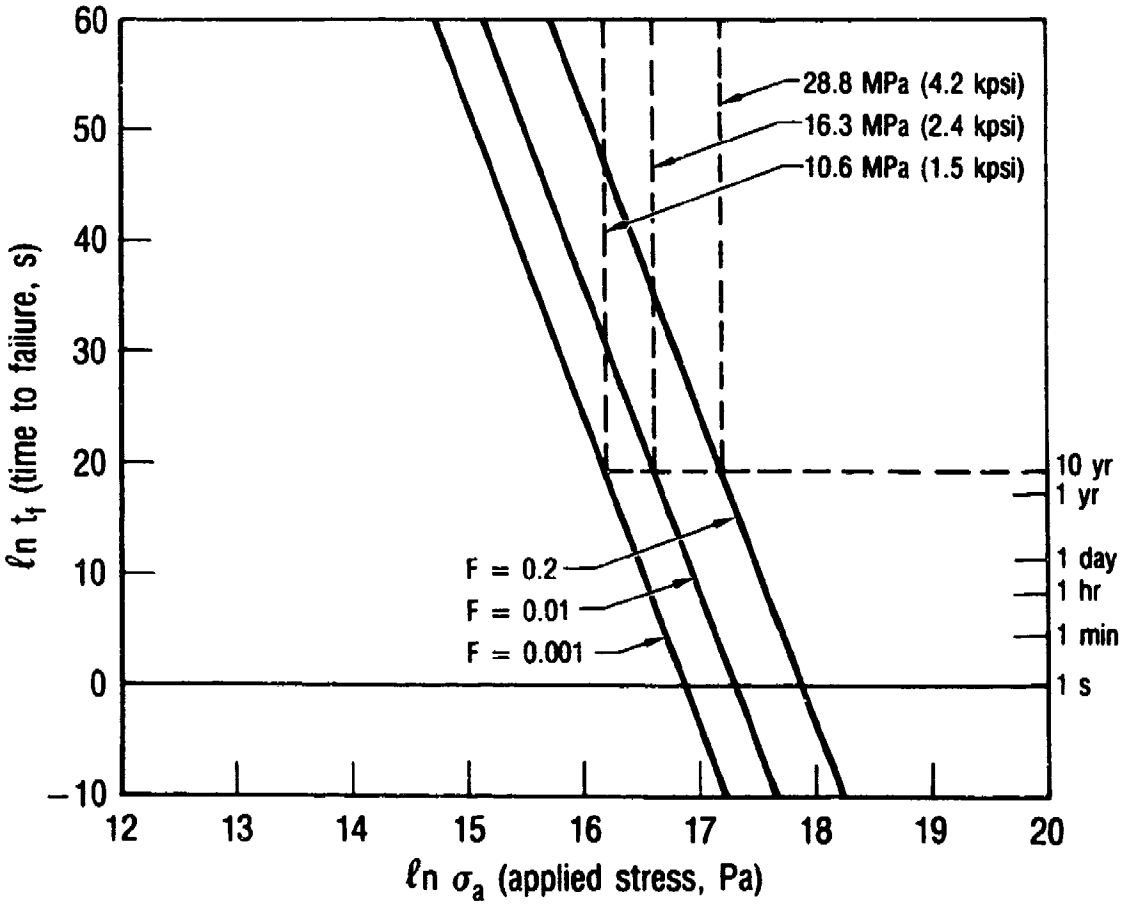

Fig. 5. Design Diagram for Polished ULE Glass, Based on Dynamic Fatigue Data

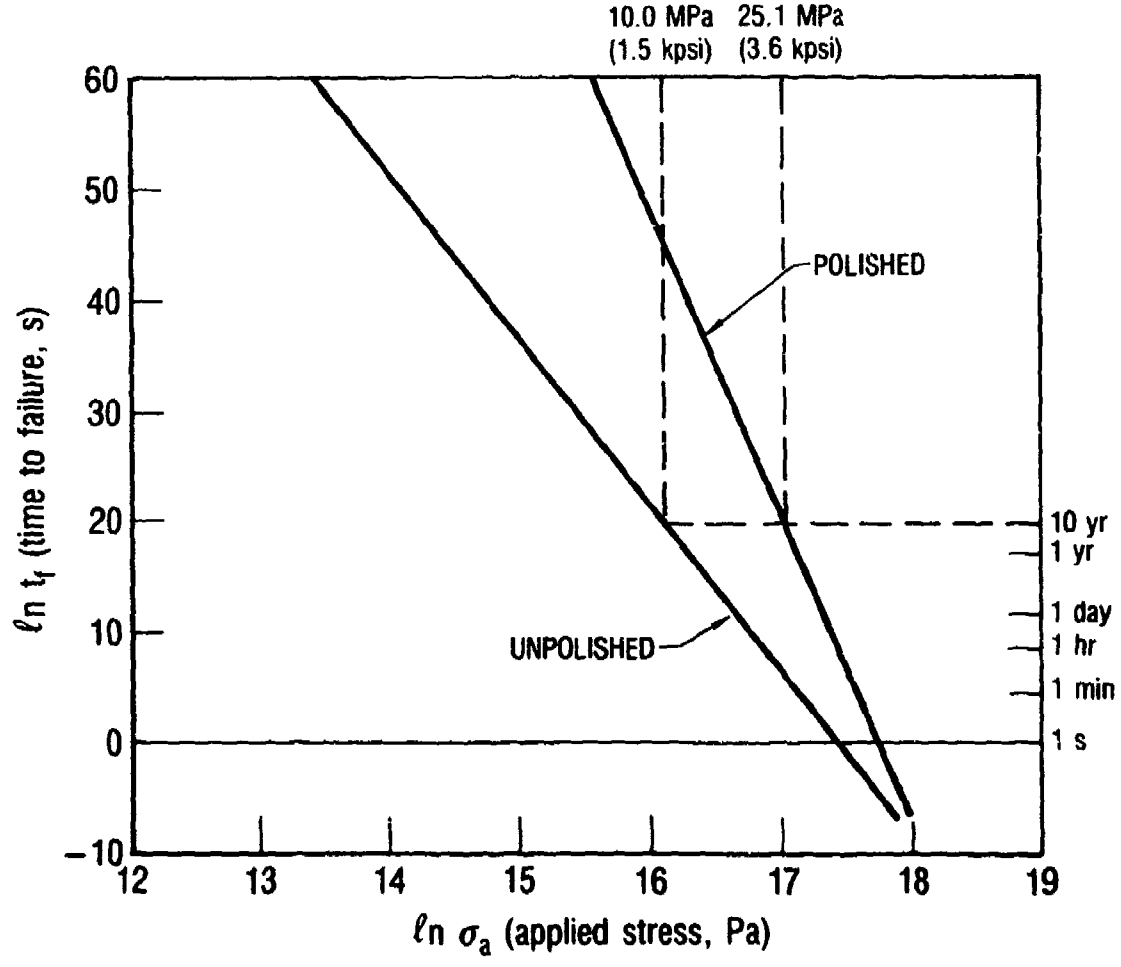

Fig. 6. Comparison of Time-to-Failure for Polished and Unpolished ULE Glass at F = 0.10

concerns how accurately the fracture data from the three-point-bend bars can be scaled to a much larger final product; this can be addressed by additional testing of large bend bars or other configurations, but has not been done here. A third factor is the reliability of the values of N and ℓn B.

In any dynamic fatigue testing, experimental uncertainty will be associated with the values of N and ℓn B. The reproducibility of these parameters can be estimated by means of a statistical approach developed by Ritter et al.;[5] any desired confidence limits can be placed on the estimated life by using the results of the statistical approach.

From the foregoing discussion it is clear that, as the flaw population changes, the sensitivity to subcritical crack growth also changes. In practice, this means that greater care should be exercised during the grinding and polishing operations than would be required for the finished blank. However, the optical requirements of the system impose a more severe set of constraints on the care that must be exercised in the handling of the finished mirror blank.

The presence of a multimode flaw distribution in these materials is a complicating factor that may affect the results.[10]

IV. SUMMARY AND CONCLUSIONS

Dynamic fatigue experiments have been carried out on polished and unpolished ultralow-expansion glass, and design diagrams have been generated for each surface condition. Subcritical crack growth has been demonstrated to occur, and the environmental parameters ln B and N vary with the surface condition. The parameter ln B varies from 31.2 to 32.2, and N varies from 15.0 to 27.9. The polished material, with an N value of 27.9, is apparently less sensitive to subcritical crack growth than the unpolished material.

If the size effects in going from three-point-bend specimens to larger structures can be determined, the design diagrams can be used in the design of ULE glass mirrors for space- and ground-based applications.

REFERENCES

1. S. M. Weiderhorn, A. G. Evans, E. R. Fuller, and H. Johnson, "Application of Fracture Mechanics to Space-Shuttle Windows," J. Amer. Ceram. Soc. 57 [7], 319-323 (1974).

2. W. Weibull, "A Statistical Theory of the Strength of Materials," Roy. Swed. Acad. of Eng. Sci. Proc. 151, 1-45 (1939).

3. J. E. Ritter, Jr., "Engineering Design and Fatigue Failure of Brittle Materials," in Fracture Mechanics of Ceramics, Vol. 4, eds. R. C. Bradt, D. P. H. Hasselman, and F. F. Lange (Plenum, New York, 1978).

4. K. K. Smyth and M. B. Magida, "Dynamic Fatigue of a Machinable Glass-Ceramic," J. Amer. Ceram. Soc. 66 [7], 500-505 (1983).

5. J. E. Ritter, Jr., N. Bandyopadhyay, and K. Jakus, "Statistical Reproducibility of the Dynamic and Static Fatigue Experiments," Bull. Amer. Ceram. Soc. 60 [8], 798-806 (1981).

6. S. M. Weiderhorn, "Mechanics of Subcritical Crack Growth in Glass," in Fracture Mechanics of Ceramics, Vol. 4, eds. R. C. Bradt, D. P. H. Hasselman, and F. F. Lange (Plenum, New York, 1978).

7. R. J. Charles, "Dynamic Fatigue of Glass," J. Appl. Phys. 29 [12], 1657-62 (1958).

8. G. S. White, D. C. Greenspan, and S. W. Freiman, "Corrosion and Crack Growth in 33% Na_2O-67% SiO_2, and 33% Li_2O-67% SiO_2 Glasses," J. Amer. Ceram. Soc. 69 [1], 38-44 (1986).

9. T. A. Michalske and S. W. Freiman, "A Molecular Mechanism for Stress Corrosion in Vitreous Silica," J. Amer. Ceram. Soc. 66 [4], 284-288 (1983).

10. C. A. Johnson, Fracture Statistics in Design and Application, General Electric Corporate R and D Report No. 79 CRD 212 (December 1979).

APPENDIX A. DERIVATION OF LIFETIME-PREDICTION EQUATIONS

The derivation of the lifetime-prediction Eq. (2) is based on expressions from fracture mechanics and Weibull statistics.[3,4] The fracture mechanics expressions describe the rate of crack growth, da/dt, in a material as a power-law function:

$$\frac{da}{dt} = AK_I^N \tag{A-1}$$

where a is the crack length, A and N are constants for a given material and environment, and K_I is the fracture toughness. The fracture toughness is related to the fracture stress σ of the material by

$$K_I = \sigma Y \sqrt{a} \tag{A-2}$$

where Y is a crack geometry parameter that is constant for a given geometry. Combining these two expressions to eliminate K_I gives

$$\frac{da}{dt} = A\, \sigma^N Y^N a^{N/2} \tag{A-3}$$

For the case of static fatigue (constant applied stress, σ_a), this expression is rewritten as

$$a^{-N/2}\, da = A\, \sigma_a^N Y^N\, dt \tag{A-4}$$

To obtain the lifetime of the material, Eq. (A-4) is integrated over the initial-to-final crack length on the left and from the time the stress was applied (t = 0) to the time at fracture, t_f, on the right. This expression thus becomes

$$\int_{a_0}^{a_f} a^{-N/2}\, da = \int_0^{t_f} A\, \sigma_a^N Y^N\, dt \tag{A-5}$$

After integration, Eq. (A-5) becomes

$$\frac{2}{N-2}\left[a_f^{-(N-2)/2} - a^{-(N-2)/2}\right] = A\,\sigma_a^{N} Y^{N} t_f \qquad \text{(A-6)}$$

Rearranging Eq. (A-2) and substituting for a gives

$$\frac{2}{N-2}\left[\left(\frac{K_{If}}{\sigma_f Y}\right)^{-(N-2)} - \left(\frac{K_{Ic}}{\sigma_0 Y}\right)^{-(N-2)}\right] = A\,\sigma_a^{N} Y^{N} t_f \qquad \text{(A-7)}$$

The fracture toughness when fracture occurs, K_{If}, is the critical fracture toughness K_{Ic}, and the fracture stress σ_f is the stress at which fracture would occur in an inert environment unaffected by subcritical crack growth σ_i. Substituting these symbols and rearranging them to obtain the time-to-failure yields

$$t_f = B\,\sigma_i^{N-2}\sigma_a^{-N} \qquad \text{(A-8a)}$$

where

$$B = \frac{2}{AY^2 K_{Ic}^{N-2}(N-2)}$$

or

$$\ln t_f = \ln B + (N-2)\ln \sigma_i - N \ln \sigma_a \qquad \text{(A-8b)}$$

Fracture of a brittle material can be regarded as a statistical process, because the material has a distribution of flaw sizes. The descriptive mathematics are by Weibull[2] and can take the forms

$$F = 1 - \exp\left(-\frac{\sigma}{\sigma_0}\right)^{m} \qquad \text{(A-9a)}$$

or

$$F = 1 - \exp\left(-\frac{\sigma - \sigma_u}{\sigma_0}^m\right) \qquad \text{(A-9b)}$$

where F is the probability that the material will fail at a stress σ, and σ_0, σ_u, and m are the descriptors of the distribution. Equation (A-9a) represents an unbounded distribution, and Eq. (A-9b) represents a lower bounded distribution. These equations implicitly contain terms in σ_0 that relate to volume or area flaw distributions.

Here, we assume we are dealing only with surface flaws, and examination of the data shows that the unbounded distribution provides a good description of the failures. Rearranging Eq. (A-9a) to obtain the fracture stress gives

$$\ln \sigma = \frac{1}{m}\left[\ln\left(\ln \frac{1}{1 - F}\right) + m \ln \sigma_0\right] \qquad \text{(A-10a)}$$

For the inert-strength distribution this expression is

$$\ln \sigma_i = \frac{1}{m_i}\left[\ln\left(\ln \frac{1}{1 - F}\right) + m_i \ln \sigma_i\right] \qquad \text{(A-10b)}$$

and substituting this expression for $\ln \sigma_i$ into Eq. (A-8b) gives

$$\ln t_f = \ln B + \frac{N - 2}{m_i}\left[\ln\left(\ln \frac{1}{1 - F}\right) + m_i \ln \sigma_{0i}\right] - N \ln \sigma_a \qquad \text{(A-11)}$$

which is Eq. (2) in the text.

APPENDIX B. MODULUS OF RUPTURE (MOR) DATA FROM THREE-POINT-BEND TESTS

Set 1: $\dot{\sigma}$ = 0.12 MPa/s; Lightly Ground, H_2O

MOR (MPa)	MOR (MPa)	MOR (MPa)
51.46	43.48	55.14
60.52	44.94	41.56
63.80	43.97	36.63
44.17	41.00	37.04
55.61	39.37	43.70
27.13	43.00	42.89
59.80	34.86	43.10
44.34	62.59	
63.89	44.88	

Set 2: $\dot{\sigma}$ = 0.12 MPa/s; Polished, H_2O

MOR (MPa)	MOR (MPa)	MOR (MPa)
67.11	68.42	47.37
79.47	76.43	36.71
70.16	79.29	38.92
88.95	66.43	36.95
46.74	37.30	74.52
67.38	53.08	71.59
74.67	73.26	78.10
48.71	66.75	
77.11	41.30	

Set 3: $\dot{\sigma}$ = 1.23 MPa/s; Lightly Ground, H_2O

MOR (MPa)	MOR (MPa)	MOR (MPa)
52.38	60.33	51.41
63.62	47.65	52.03
41.20	44.89	46.32
38.60	42.46	43.90
43.66	44.14	44.12
50.50	37.25	43.57
37.44	42.46	45.45
63.85	37.17	
62.91	63.90	

Set 4: $\dot{\sigma}$ = 1.23 MPa/s; Polished, H_2O

MOR (MPa)	MOR (MPa)	MOR (MPa)
85.33	80.28	75.97
74.68	86.04	86.81
78.58	74.85	89.47
88.17	64.78	60.47
61.23	84.32	63.42
76.59	68.87	83.42
48.44	66.03	91.39
97.06	75.55	
47.24	79.69	

Set 5: $\dot{\sigma}$ = 12.3 MPa/s; Lightly Ground, H_2O

MOR (MPa)	MOR (MPa)	MOR (MPa)
60.67	64.53	55.51
62.53	60.88	62.40
57.42	59.45	59.09
63.09	42.90	56.21
58.13	42.88	67.23
57.89	61.07	44.28
59.84	58.72	52.92
48.11	46.92	
65.71	67.06	

Set 6: $\dot{\sigma}$ = 12.3 MPa/s; Polished, H_2O

MOR (MPa)	MOR (MPa)	MOR (MPa)
40.31	76.42	84.12
54.24	83.58	85.54
65.23	86.53	72.71
71.31	81.40	53.97
77.86	64.29	84.19
79.70	56.12	92.71
52.83	94.09	91.49
92.03	43.54	
90.39	89.75	

Set 7: $\dot{\sigma}$ = 12.3 MPa/s; Lightly Ground, N_2

MOR (MPa)	MOR (MPa)	MOR (MPa)
50.74	69.76	52.31
36.52	82.27	71.71
58.49	53.28	59.85
70.44	77.83	53.90
52.68	74.97	51.87
72.85	68.71	79.83
79.54	73.97	48.68
65.03	45.39	
50.03	67.10	

Set 8: $\dot{\sigma}$ = 12.3 MPa/s; Polished, N_2

MOR (MPa)	MOR (MPa)	MOR (MPa)
108.08	74.16	93.28
116.70	107.74	71.37
105.25	83.25	107.14
83.38	96.74	83.72
97.62	103.98	79.95
62.42	98.34	56.20
82.79	109.10	53.02
51.14	67.25	
88.41	65.63	

Set 9: $\dot{\sigma}$ = 147 MPa/s; Lightly Ground, N_2

MOR (MPa)	MOR (MPa)
63.32	81.42
61.56	61.62
75.55	72.34
73.10	76.47
72.94	78.97
66.45	69.71
69.30	59.01

Set 10: $\dot{\sigma}$ = 347 MPa/s; Lightly Ground, N_2

MOR (MPa)	MOR (MPa)
55.65	51.80
68.08	56.74
73.33	54.69
47.08	71.99

LABORATORY OPERATIONS

The Aerospace Corporation functions as an "architect-engineer" for national security projects, specializing in advanced military space systems. Providing research support, the corporation's Laboratory Operations conducts experimental and theoretical investigations that focus on the application of scientific and technical advances to such systems. Vital to the success of these investigations is the technical staff's wide-ranging expertise and its ability to stay current with new developments. This expertise is enhanced by a research program aimed at dealing with the many problems associated with rapidly evolving space systems. Contributing their capabilities to the research effort are these individual laboratories:

Aerophysics Laboratory: Launch vehicle and reentry fluid mechanics, heat transfer and flight dynamics; chemical and electric propulsion, propellant chemistry, chemical dynamics, environmental chemistry, trace detection; spacecraft structural mechanics, contamination, thermal and structural control; high temperature thermomechanics, gas kinetics and radiation; cw and pulsed chemical and excimer laser development including chemical kinetics, spectroscopy, optical resonators, beam control, atmospheric propagation, laser effects and countermeasures.

Chemistry and Physics Laboratory: Atmospheric chemical reactions, atmospheric optics, light scattering, state-specific chemical reactions and radiative signatures of missile plumes, sensor out-of-field-of-view rejection, applied laser spectroscopy, laser chemistry, laser optoelectronics, solar cell physics, battery electrochemistry, space vacuum and radiation effects on materials, lubrication and surface phenomena, thermionic emission, photosensitive materials and detectors, atomic frequency standards, and environmental chemistry.

Computer Science Laboratory: Program verification, program translation, performance-sensitive system design, distributed architectures for spaceborne computers, fault-tolerant computer systems, artificial intelligence, microelectronics applications, communication protocols, and computer security.

Electronics Research Laboratory: Microelectronics, solid-state device physics, compound semiconductors, radiation hardening; electro-optics, quantum electronics, solid-state lasers, optical propagation and communications; microwave semiconductor devices, microwave/millimeter wave measurements, diagnostics and radiometry, microwave/millimeter wave thermionic devices; atomic time and frequency standards; antennas, rf systems, electromagnetic propagation phenomena, space communication systems.

Materials Sciences Laboratory: Development of new materials: metals, alloys, ceramics, polymers and their composites, and new forms of carbon; nondestructive evaluation, component failure analysis and reliability; fracture mechanics and stress corrosion; analysis and evaluation of materials at cryogenic and elevated temperatures as well as in space and enemy-induced environments.

Space Sciences Laboratory: Magnetospheric, auroral and cosmic ray physics, wave-particle interactions, magnetospheric plasma waves; atmospheric and ionospheric physics, density and composition of the upper atmosphere, remote sensing using atmospheric radiation; solar physics, infrared astronomy, infrared signature analysis; effects of solar activity, magnetic storms and nuclear explosions on the earth's atmosphere, ionosphere and magnetosphere; effects of electromagnetic and particulate radiations on space systems; space instrumentation.